DOI 10.1007/s11182-023-03059-z
Russian Physics Journal, Vol. 66, No. 11, January, 2024

PHYSICAL AND MECHANICAL PROPERTIES OF MULTICOMPONENT (Zr+TiBSiNi)N COATING FABRICATED BY PLASMA-ASSISTED VACUUM-ARC DEPOSITION

V. M. Savostikov,[1] A. A. Leonov,[1] V. V. Denisov,[1] Yu. A. Denisova,[1] M. V. Savchuk,[1] A. B. Skosyrskii,[1,2] and A. N. Shmakov[1,3]

UDC 621.793.14, 537.525

The paper studies physical and mechanical properties of multicomponent (Zr+TiBSiNi)N *coating synthesized by vacuum-arc deposition using the traditional plasma-assisted gas source "PINK" and new beam-plasma formation (BPF) system. It is shown that the coating obtained by using the BPF system, has better properties that the coating obtained by using the traditional plasma-assisted gas source. In the first case, the coating hardness is 47.8 GPA and in the second case, it is 40.9 GPa. The X-ray diffraction analysis shows that along with* ZrN *and* TiN *phases, the BPF-synthesized coating consists of the superhard and heat-resistant* TiB_2 *phase. The X-ray diffraction analysis of the phase composition conducted for the in situ synchrotron radiation beam, shows that notable phase transformations start at temperatures higher than 750°C.*

Keywords: vacuum arc deposition, multicomponent coating, beam-plasma formation, gas discharge plasma, microhardness, X-ray diffraction analysis.

INTRODUCTION

Simple ZrN coatings are not widely used as wear resistant in the tool production owing to their lower hardness as compared to conventional and widespread TiN coatings [1–3]. However, ZrN oxidation resistance higher than TiN, is interesting to researchers and developers of technologies [4]. There is a tendency to the creation of ZrN coatings together with other elements and compositions with a view to improve their physical and mechanical properties [5–7]. For example, in our research [8], the oxidation resistance of the ZrN coating is improved due to a combination of the ZrN/CrN compound. Sobol *et al*. [9] report that the difference between ZrN/CrN and TiN/CrN coatings is the higher resistance of the former to radiation damage. This assertion causes the additional interest for using ZrN/CrN coatings in nuclear industry [10, 11]. In particular fuel element shells operating at 650–700°C, are subjected to corrosion induced by overheated water [12]. Hence, protective coatings must provide high-temperature (>700 °C) resistance to oxidation. It is interesting to note that Beresnev *et al*. [13] find that at 500°C, Zr-Ti-Si-N coatings possess the higher wear resistance and lower coefficient of friction than TiN and Ti-Si-N coatings.

The aim of this work is to investigate physical and mechanical properties of plasma-assisted vacuum-arc deposition of the (Zr+TiBSiNi)N coating consisting of above indicated elements. The paper gives a comparison for two plasma-assisted methods, *sc*. the relatively novel beam-plasma formation (BPF) system [14] and conventional plasma-assisted gas source "PINK" [15, 16].

[1]Institute of High Current Electronics of the Siberian Branch of the Russian Academy of Sciences, Tomsk, Russia, e-mail: svm.53@mail.ru; laa-91@yandex.ru;, denisov@opee.hcei.tsc.ru; yudenisova81@yandex.ru; mixail96@bk.ru; [2]National Research Tomsk State University, Tomsk, Russia, e-mail: qwert1902@rambler.ru; [3]Budker Institute of Nuclear Physics of the Siberian Branch of the Russian Academy of Sciences, Novosibirsk, Russia, e-mail: highres@mail.ru. Original article submitted November 9, 2023.

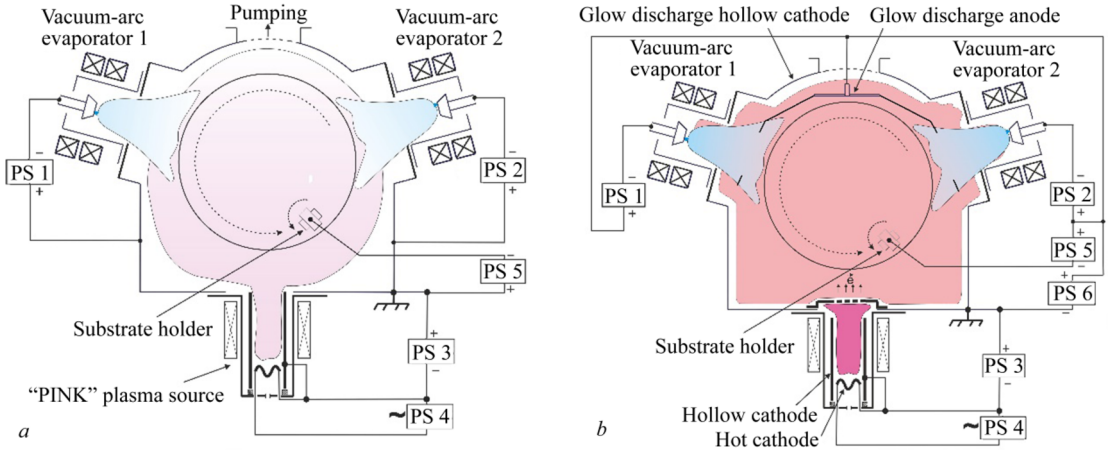

Fig. 1. Schematic views of the plasma-assisted vacuum-arc deposition system: *a* – traditional "PINK" plasma source, *b* – new beam-plasma formation in hot cathode arc discharge plasma.

MATERIALS AND METHODS

The plasma-assisted vacuum-arc deposition of the (Zr+TiBSiNi)N coating is performed on the upgraded system Bulat NNV6.6-I1 (Russia) equipped with the additional different plasma sources [17]. The schematic view of this coating deposition system is presented in Fig. 1. In the traditional configuration of the plasma generation (Fig. 1*a*), the plasma source "PINK" is used to produce the plasma concentration gradient directed towards the chamber walls. Its maximum concentration locates nearby the "PINK" exit aperture, while the minimum concentration locates at a distance from it. The maximum density of metal plasma flows created by vacuum-arc evaporators, is observed nearby cathodes. Apparently, this nonuniform distribution of gas and metal ion flows affects the results reproducibility and coating properties. This is especially important for large-sized products and/or in real production conditions, when it is necessary to provide uniform properties for obtained products on different areas of the working surface.

The coating was deposited onto cylindrical substrates with the diameter 8 mm and 6 mm high, made of the WC–8Co alloy. These substrates were mounted to the turning table to simulate the real arrangement of tools for the coating deposition in production conditions. During sputtering, the cylinders rotated about themselves and circumferentially relative to vacuum-arc evaporators and gas plasma source (Fig. 1). The rotation speed of the turning table was 3.5 rpm.

For comparison, two vacuum-arc evaporators with 80 mm cylindrical cathodes were used in both cases to generate the solid-state plasma. Cathodes were prepared by SHS pressing of the Ti-B-Si-Ni system and E-110 zirconium alloy consisting of 0.9 to 1.1% Nb. SHS cathodes were fabricated from exothermic combination of Ti, B, Si elements taken respectively in the atomic ratio 2:2:1 with the introduction of 10 at.% Ni as a binder [18]. Argon or nitrogen gas plasma generated by the "PINK" source or in the beam-plasma formation, was used to preliminary clean the surface of products from dielectric and oxide films using the ion bombardment and also assisted in the coating synthesis. Cylindrical substrates were cleaned and heated in argon gas discharge plasma at a higher negative bias voltage of 900 V. The additional vacuum-arc evaporator with the Zr cathode was connected to the system for the substrate heating and diffusion of sputtered solid elements onto its surface, i.e., for the improvement of the substrate adhesion to the bonding sublayer of the coating. The bonding sublayer was deposited with evaporation of respective cathodes in argon at 150 V bias voltage and 3 min deposition time. The coating was deposited at 150 V bias voltage of the substrate in a mixture of N_2 and Ar in the proportion of 90 to 10, respectively. The deposition temperature of next coatings was 420°C. The arc discharge current was 60 A (minimized for the droplet fraction reduction) for the Zr

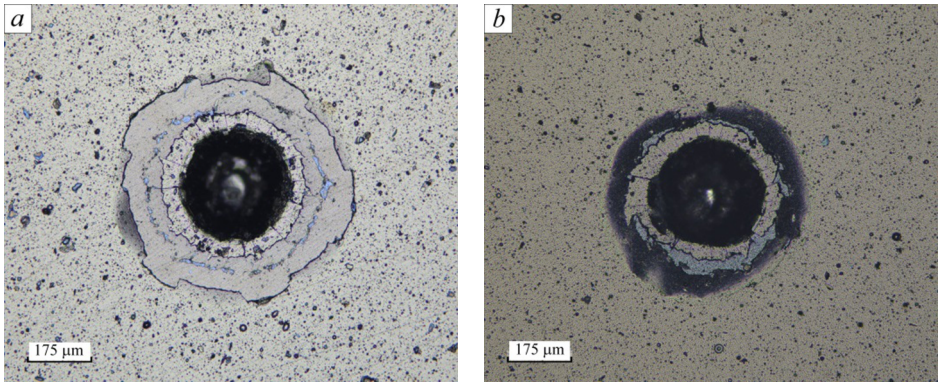

Fig. 2. Rockwell hardness test results of (Zr+TiBSiNi)N coatings: *a* – using "PINK" plasma source, *b* – using BPF system.

cathode and 80 A for the Ti-B-Si-Ni cathode. The total pressure in the chamber was 0.6 Pa during the deposition process, and the depositшon time was 90 min.

Actual coating thickness was studied first by Calotest techniques and then by the KBW-1 microhardness tester (KB Pruftechnik GmbH, Germany) using Vickers pyramid diamond indentation at 0.1 N load. Each coating was tested at 10 points, and the obtained results were averaged. The adhesive strength and brittleness were measured for all coatings using three Rockwell-C indentation tests at 1500 N load. A Revetest scratch tester (CSM Instruments, USA) equipped with a Rockwell C diamond stylus, was used to measure the coating adhesion to the substrate, and the acoustic emission signal was recorded depending on the indentation load. The latter increased linearly from zero to 150 N. A DMi8M Inverted Microscope (Leica Microsystems, Germany) was used to investigate the surface scratch. The phase composition of the coatings was investigated on a Shimadzu XRD-6000S Diffractometer using Cu Kα radiation. The analysis of the phase composition was performed using PDF4+ database and the Crystallographica Search-Match program. After the preliminary analysis of results demonstrating the high efficiency of the traditional "PINK" plasma source, X-ray diffraction (XRD) analysis of phase transformations in the coating was conducted using the synchrotron radiation beam at the specimen heating in air up to 1100°C. The experiment was conducted on an *in situ* diffractometer of the "Precise Diffractometry II" beamline mounted on channel No. 6 of the VEPP-3 storage ring in Siberian Synchrotron and Terahertz Radiation Centre of the Budker Institute of Nuclear Physics SB RAS, Novosibirsk, Russia. The substrate was heated in the HTK 2000 (Anton Paar) high temperature chamber using a platinum heater also served as the substrate holder. The process parameters included 0.172 nm wavelength, 15°C/min heating rate, 30 to 1100°C temperature range. XRD patterns were recorded by the position sensitive detector OD-3M-350 at the exposure time of 1 min. Fityk (1.3.1) program was used for the obtained data processing.

RESULTS AND DISCUSSION

The thickness and microhardness of the (Zr+TiBSiNi)N coating synthesized by the "PINK" plasma source, were 3.9 μm and 40.9 GPa, respectively. Along with the ion bombardment from the "PINK" plasma source, this high hardness could be explained by the multilayer coating structure due to alternating substrate pass through the evaporation zone on cathodes having different composition. The calorimetric analysis of the BPF-synthesized coating, showed its 3 μm thickness, which was slightly lower than the thickness (3.9 μm) of the coating obtained by the traditional plasma source. This could be conditioned by more intensive evaporation of deposited atoms from the BPF system than from the "PINK" plasma source. But the microhardness of this coating notably grew up to 47.8 GPa as compared to the microhardness 40.9 GPa obtained for "PINK"-synthesized coatings. The Rockwell hardness test in Fig. 2, shows the (Zr+TiBSiNi)N coating delamination, which was obtained in the gas and metal beam-plasma formation. Unlike the "PINK"-synthesized coating, this delamination is not leaf-like on the periphery. The difference between the outer and

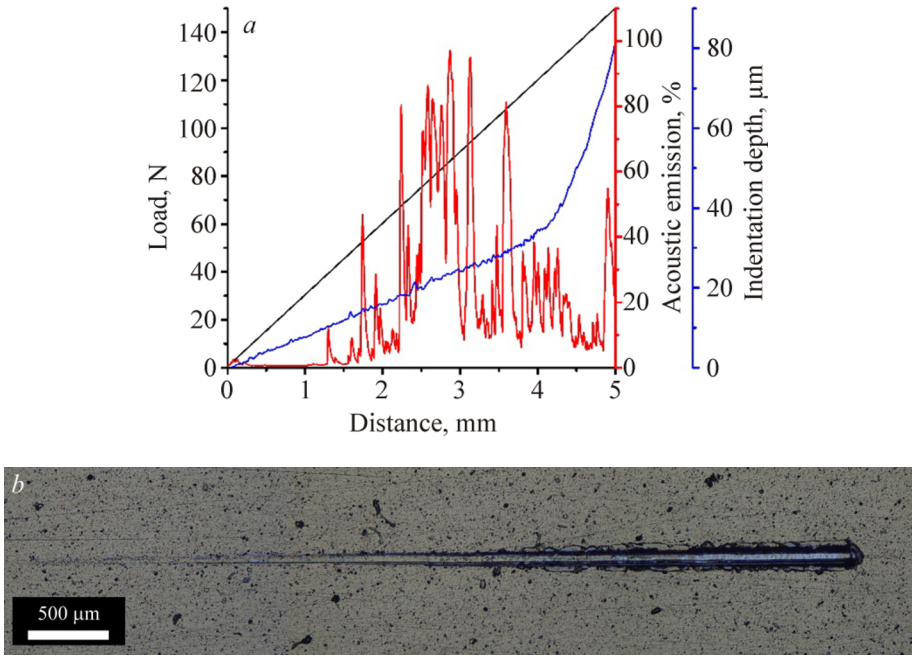

Fig. 3. Dependence of the acoustic emission signal on the indentation load and depth during scratch tests of "PINK"-synthesized coating (Zr+TiBSiNi)N (*a*), photograph of the wear track (*b*).

inner diameters of the coating delamination, is 1.7, while for the coating obtained with use of the "PINK", this difference comes to 2.0. This indirectly indicates to the better adhesion of the BPF-obtained coating to the substrate.

Figure 3*a* presents the dependence of the acoustic emission signal on the indentation load and depth during scratch tests of "PINK"-synthesized coatings, and Fig. 3*b* shows the wear track. The dependence between the acoustic emission signal and the indentation depth, is linear up to 50 N load. At a 1.5 mm depth from the surface, there are acoustic emission peaks, although the coating is not yet worn (Fig. 3*a*, *b*). This indicates to elastic deformation induced by the indenter and cohesive wear of the coating surface.

The dependence shown in Fig. 4*a*, is typical for the acoustic emission signal from the indenter penetration load and depth during scratch tests of the BPF-synthesized coating. Figure 4*b* presents the photograph of the obtained wear track.

The dependence between the acoustic emission signal and the indentation depth, is linear up to 80 N load. At a 2.5 mm depth from the surface, the acoustic emission signal decays. The coating delamination from the substrate starts at a 4 mm distance, that exceeds values obtained for the "PINK"-synthesized coating and indicates to its better adhesion to the substrate.

XRD patterns in Fig. 5 show the difference between the phase compositions of the "PINK"- and BPF-obtained (Zr+TiBSiNi)N coatings. One can see a great difference between the phase composition of the obtained coatings. The (Zr+TiBSiNi)N coating synthesized in the beam-plasma formation, consists of titanium borides and silicides (TiB_2 and $TiSi_2$) possessing the higher thermal stability than titanium and zirconium nitrides. These phases probably provide the high integral hardness for the whole coating [19, 20].

According to the data obtained, we expect that the new method of the (Zr+TiBSiNi)N coating synthesis in the beam-plasma formation is more effective than in the traditional gas and metal plasma generation. Additional X-ray diffraction studies (Fig. 6) are performed for the (Zr+TiBSiNi)N coating using synchrotron radiation during heating in air. It is found that notable phase transformations begin at 750°C, in particular the ZrO_2 phase formation is observed. In general, this denotes the high thermal stability of the synthesized multicomponent coating (Zr+TiBSiNi)N.

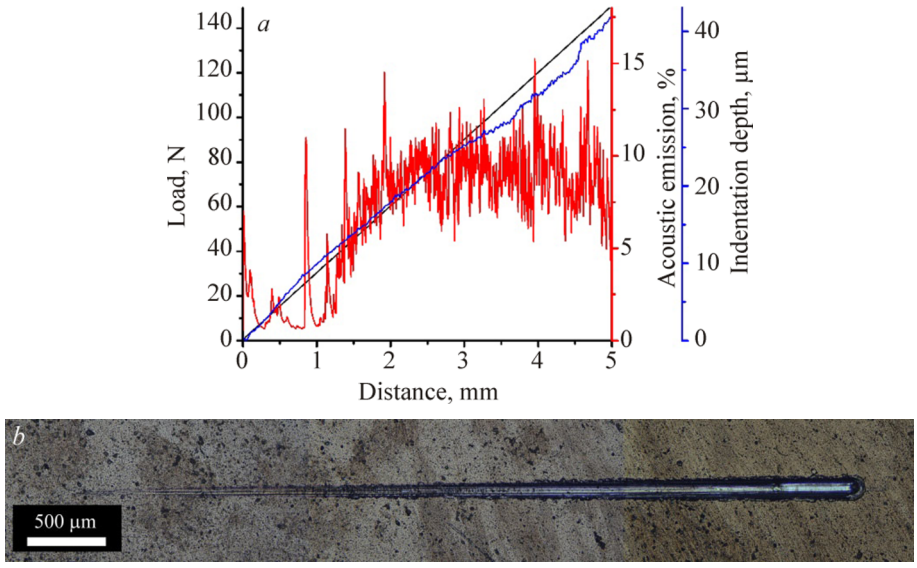

Fig. 4. Dependence of the acoustic emission signal on the indentation load and depth during scratch tests of BPF-synthesized coating (Zr+TiBSiNi)N (*a*), photograph of the wear track (*b*).

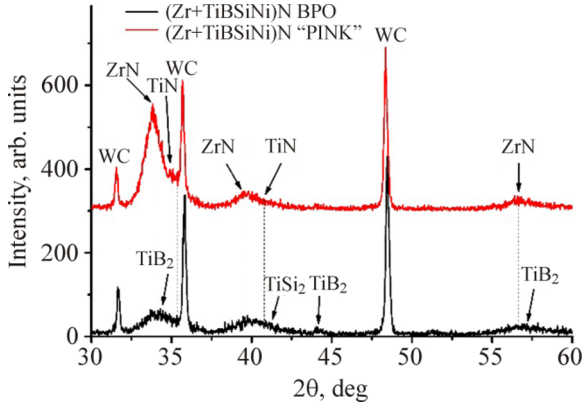

Fig. 5. XRD patterns for the phase compositions of "PINK"- (top) and BPF-synthesized (bottom) (Zr+TiBSiNi)N coatings.

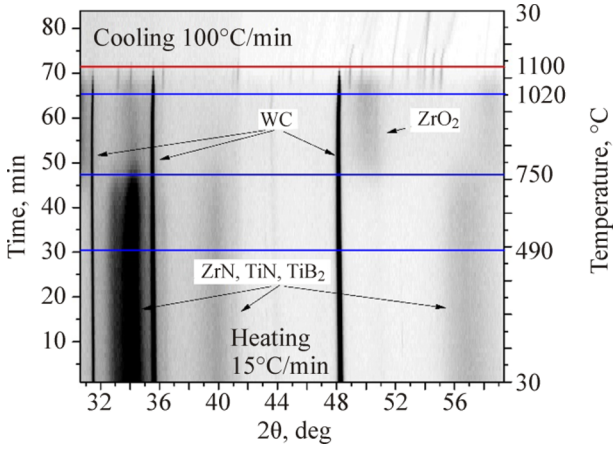

Fig. 6. *In situ* XRD analysis.

CONCLUSIONS

A comprehensive analysis of the multicomponent coating (Zr+TiBSiNi)N properties confirmed the high efficiency of its formation in gas and metal beam-plasma formation, rather than in the traditional gas-metal plasma generation by the "PINK" source. Most likely, that resulted from the uniform and constant influence of the reaction gas ions on the deposited coating layers, and hence a higher probability of formation of necessary functional compounds in it. The obtained data on the high (>40 GPa) hardness of the (Zr+TiBSiNi)N coating synthesized in the new discharge system and a good combination of the coating high hardness and sufficient adhesion to the substrate, suggested the possibility of its use for hardening cutting tools for hard-to-machine materials, in particular, hardened steels and alloys.

COMPLIANCE WITH ETHICAL STANDARDS

Conflicts of interest

The authors declare no conflict of interest.

Funding

Research was financially supported by the Ministry of Science and Higher Education of the Russian Federation (Project No. 075-15-2021-1348).

Financial interests

The authors declare they have no financial interests.

Non-financial interests

None.

REFERENCES

1. A. A. Vereshchaka, Vestnik Brianskogo gosudarstvennogo tekhnicheskogo universiteta, **4**, No. 48, 25 (2015); DOI: 10.12737/17077.
2. T. M. Cholakova, L. P. Kolaklieva, Hr. P. Bahchedjiev, R. D. Kakanakov, B. Ranguelov, and N. T. Hristeva, J. Phys.: Conf. Ser., **1492**, 012036 (2020); DOI: 10.1088/1742-6596/1492/1/012036.
3. A. A. Ashmarin, S. Ya. Betsofen, L. M. Petrov, and M. A. Lebedev, IOP Conf. Ser.: Mater. Sci. Eng., **889**, 012019 (2020); DOI: 10.1088/1757-899X/889/1/012019.
4. C. Ziebert and S. Ulrich, J. Vac. Sci. Technol. A, **24**, 554 (2006); DOI: 10.1116/1.2194031.
5. T. A. Kuznetsova, V. A. Lapitskaya, S. A. Chizhik, B. Warcholinski, A. Gilewicz, and A. S. Kuprin, IOP Conf. Ser.: Mater. Sci. Eng., **443**, 012017 (2018); DOI 10.1088/1757-899X/443/1/012017.
6. M. Yin, W. Liang, Q. Miao, and H. Yu, Ceram. Int., **47**, 34085 (2021); DOI: 10.1016/j.ceramint.2021.08.317.
7. J. Musil, P. Zeman, H. Hrubý, and P. H. Mayrhofer, Surf. Coat. Technol., 120–121, 183 (1999); DOI: 10.1016/S0257-8972(99)00482-X.
8. A. Vorontsov, A. Filippov, N. Shamarin, E. Moskvichev, O. Novitskaya, E. Knyazhev, Y. Denisova, A. Leonov, V. Denisov, and S. Tarasov, Metals, **12**, 1746 (2022); DOI: 10.3390/met12101746.

9. O. V. Sobol, A. A. Andreev, V. F. Gorban, A. A. Meilekhov, A. A. Postelnik, and V. A. Stolbovoi, J. Nano-Electron. Phys., **8**, 01042 (2016); DOI: 10.21272/jnep.8(1).01042.
10. F. Khatkhatay, J. Jian, L. Jiao, Q. Su, J. Gan, J. I. Cole, and H. Wang, J. Alloys Compd., **580**, 448 (2013); DOI: 10.1016/j.jallcom.2013.06.108.
11. S. Bhattacharya, L. Jamison, D. N. Seidman, W. Mohamed, Y. Bei, M. J. Pellin, and A. M. Yacout, J. Nucl. Mater., **526**, 151770 (2019); DOI: 10.1016/j.jnucmat.2019.151770.
12. E. L. Vardanyan, K. N. Ramazanov, R. Sh. Nagimov, and A. Yu. Nazarov, Surf. Coat. Technol., **389**, 125657 (2020); DOI: 10.1016/j.surfcoat.2020.125657.
13. V. M. Beresnev, V. V. Grudnitskii, U. S. Nemchenko, M. V. Kaverin, A. M. Makhmud, G. V. Kirik, M. Y. Smolyakova, D. A. Kolesnikov, and F. F. Komarov, J. Frict. Wear, **33**, 173 (2012); DOI: 10.3103/S1068366612030026.
14. V. V. Denisov, Y. A. Denisova, E. L. Vardanyan, E. V. Ostroverkhov, A. A. Leonov, and M. V. Savchuk, Russ. Phys. J., **64**, 150 (2021); DOI: 10.1007/s11182-021-02310-9.
15. A. S. Grenadyorov, K. V. Oskomov, A. A. Solovyev, N. M. Ivanova, and V. S. Sypchenko, Russ. Phys. J., **62**, 1206 (2019). DOI: 10.1007/s11182-019-01835-4.
16. A. I. Menshakov, D. R. Emlin, N. V. Gavrilov, Yu. S. Surkov, and S. O. Cholakh, Izv. Vyssh. Uchebn. Zaved., Fiz., **61**, 172 (2018).
17. A. A. Leonov, Y. A. Denisova, V. V. Denisov, M. S. Syrtanov, A. N. Shmakov, V. M. Savostikov, and A. D. Teresov, Coatings, **13**, 351 (2023); DOI: 10.3390/coatings13020351.
18. V. M. Savostikov, A. A. Leonov, V. V. Denisov, Yu. A. Denisova, A. B. Skosyrsky, and I. A. Shulepov, J. Surf. Investig., **17**, 686 (2023); DOI: 10.1134/S102745102303031X.
19. F. Movassagh-Alanagh, A. Abdollah-Zadeh, M. A. Zolbin, N. Nemati, and R. Aghababaei, Tribol. Int., **179**, 108137 (2013); DOI: 10.1016/j.triboint.2022.108137.
20. L. Yu, H. Luo, J. Bian, H. Ju, and J. Xu, Coatings, **7**, 137 (2017); DOI: 10.3390/coatings7090137.